



US Army Corps  
of Engineers®

# Model for the Computation of Time-Steady Nearshore Currents

by *Bradley Johnson*

---

**PURPOSE:** The Coastal and Hydraulics Engineering Technical Note (CHETN) herein introduces a new model for the computation of depth-dependent time-steady currents in the surf zone.

**BACKGROUND:** Under the assumptions of longshore uniformity, monochromatic and unidirectional waves, one-dimensional (1-D) models have predicted the steady depth-integrated longshore current with reasonable accuracy in the regions of intense breaking (e.g., Bowen 1969; Longuet-Higgins 1970; Kraus and Larsen 1991). The addition of random wave fields with directional spread (Battjes 1974; Thornton and Guza 1986) produce similar results but indicate a difference in the magnitude of the horizontal mixing terms. It is, however, necessary to also predict the vertical structure of time-steady currents in the surf zone to reliably compute sediment transport rates. Indeed, concentrations of sediment are found to be orders of magnitude larger in the near-bed boundary layer where fluid velocities are, in general, smaller than the depth-averaged value. It is, therefore, of practical importance to predict the vertical variation of nearshore currents.

The phase resolving equations of fluid motion may be best suited for a physically based prediction of sediment transport. Lin and Liu (1998), for instance, solved the Reynolds equations with an algebraic nonlinear Reynolds stress model. Karambas and Koutitas (2002) and Kobayashi and Johnson (2001) used Boussinesq and nonlinear shallow-water formulations, respectively. These time-dependent numerical models, however, are not suitable to most practical engineering problems due to the prohibitively large computation time.

The new model **NEARHYDS** efficiently predicts wave height, setup, bed ripple formation, boundary layer thickness, and depth-dependent steady cross-shore and longshore currents. The solution of the time-averaged equations of energy balance and alongshore momentum is implemented with modular coding that is flexible and well suited for the iterative process required to include the effects of interaction. **NEARHYDS** is a compiled collection of Matlab routines and a graphical user interface complete with an on-line user's guide and is suitable for the computation of steady nearshore hydrodynamics on beaches with essentially straight and parallel contours. The compiled version runs on a Windows PC, and the hydrodynamic predictions for a typical surf zone domain are completed in several seconds. This physics-based two-dimensional (2-D) model has been funded through the Advanced Nearshore Circulation work unit of the U.S. Army Corps of Engineers Navigation Systems Research Program and will form the basis for a more general version that allows alongshore variability.

No mechanism exists within the formulation of the equations for the generation of low-frequency standing or progressive waves in the cross-shore. These low frequency motions, however, may play an important role in cross-shore profile development. While the wave-current interaction is included in the bottom boundary layer and stress analysis, the effect of the currents on the short waves was

not considered. As justification, it was found that the deviation from Snell's law due to longshore current is exceedingly small, and the cross-shore currents are considered to be small relative to the wave phase speed on alongshore uniform coasts.

**MODEL DESCRIPTION:** The decay in wave height of obliquely incident waves is the primary generation mechanism for longshore currents; undertow is generated through the mass flux due to the presence of waves, a surface roller, and the depth-inhomogeneity of the radiation stress. Wave breaking is incorporated into the momentum equations through the solution of a suitable phase-averaged energy equation in the cross-shore direction. With an estimate of the energy flux, the radiation stresses due to the organized wave motions can be quantified and included as forcing in the time-averaged and depth-averaged momentum equations. The gradients of the radiation stress in the cross-shore direction are counteracted, primarily, by a slope in the mean free surface position, termed the setup. The alongshore momentum equation is a balance of the radiation stress gradient with momentum mixing and bottom shear stress. The depth-variation of the steady currents are based on horizontal time-averaged Reynolds equations where use is made of the solutions of the energy and depth-integrated momentum equations as well as physically-based closures. First, the solution of the phase-averaged energy equation for the waves is presented, where two approaches are provided: a root-mean-square (RMS) representation and a wave-by-wave (WBW) representation. Comparisons of wave height are presented as verification of these methods. Second, the solution of the cross-shore momentum balance is described, and results in the predictions of setup and steady cross-shore currents. Finally, the longshore momentum balance is presented that provides the longshore current. Comparisons with lab data are shown as a gauge of the model accuracy, and more thorough validation with field data will be completed as the development process proceeds.

**Phase-Averaged Energy Equation.** The energy equation, time-averaged over many short wave periods, may be expressed as

$$\frac{d}{dx} \overline{E_F} = -\overline{D_B} \quad (1)$$

in which  $x$  is the cross-shore coordinate positive onshore;  $\overline{E_F}$  = time-averaged energy flux per unit width; and  $\overline{D_B}$  = time-averaged energy dissipation rate due to wave breaking, which needs to be estimated empirically in this model. The model **NEARHYDS** solves Equation 1 with either the RMS wave height representation presented by Battjes and Jansen (1978) and calibrated by Battjes and Stive (1985) or expressed as the superposition of regular waves (WBW) (e.g., Dally 1992).

**RMS representation.** The time-averaged energy flux per unit width for random waves can be represented with the RMS wave height and peak period as

$$\overline{E_F} = \frac{1}{8} \rho g H_{rms}^2 n C_p \cos \alpha \quad (2)$$

where  $\rho g$  is the unit weight of water;  $H_{rms} = \sqrt{8} \sigma$  with  $\sigma$  = standard deviation of the free-surface elevation;  $n$  is the ratio of the wave group speed to linear phase speed;  $C_p$  = phase velocity based on  $T_p$ ; and  $\alpha$  = spectral peak angle (Figure 1).

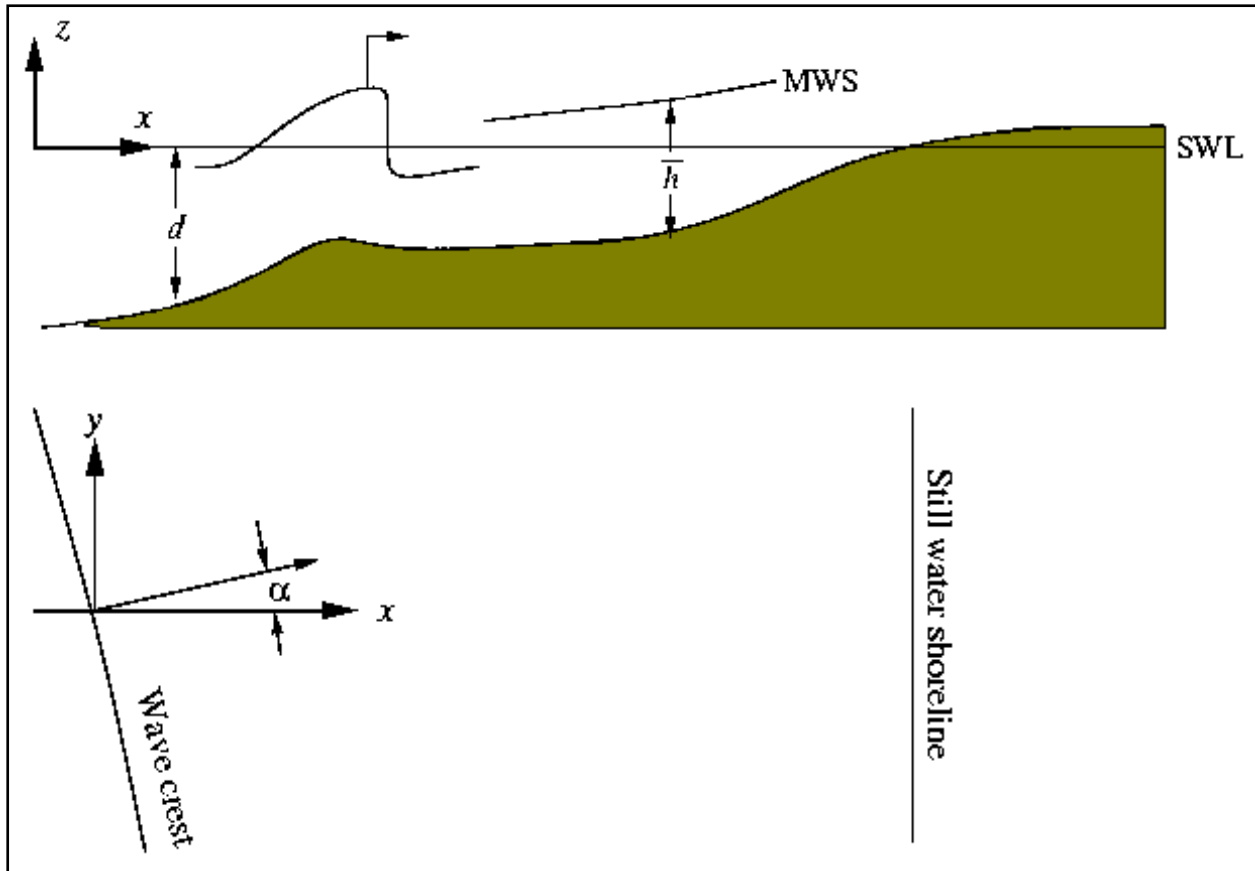


Figure 1. Variable definition sketch

The wave breaking dissipation formula by Battjes and Stive (1985) is given by

$$\overline{D_B} = \frac{1}{4} \rho g f_p Q H_m^2 \quad (3)$$

where  $f_p$  is the spectral peak frequency ;  $Q$  is the local fraction of breaking waves governed by a Rayleigh wave height distribution truncated with the maximum wave height  $H_m$  determined using the Miche criteria.

The energy equation (1) is integrated numerically using Equations 2 and 3, resulting in an estimate of the cross-shore distribution of wave height. Recalling that the energy equation is the first step in the solution of the time-averaged momentum balance, the radiation stresses are then expressed using linear theory as

$$S_{xx} = \frac{1}{8} \rho g H_{rms}^2 \left[ n(\cos^2 \alpha + 1) - \frac{1}{2} \right] ; \quad S_{xy} = \frac{1}{8} \rho g H_{rms}^2 n \sin \alpha \cos \alpha \quad (4)$$

**Linear wave superposition method.** Alternatively, the energy flux can be expressed as the superposition of monochromatic waves under the assumption of narrow bandedness in frequency. Individual wave contributions are governed by

$$\overline{E}_{Fi} = \frac{1}{8} \rho g H_i^2 n C_p \cos \alpha \quad i = 1 : N \quad (5)$$

where  $H_i$  = wave height for the  $i^{th}$  wave, and  $N$  is the total number of waves. The values of each wave height realization at the offshore boundary are given in terms of the exceedance probability  $P_e$

$$H_i = H_{rms} \sqrt{\ln \left( \frac{1}{P_{e_i}} \right)} \quad i = 1 : N \quad (6)$$

where  $P_{e_i}$  is a single realization of the random variable  $P_e$  that is uniformly distributed between zero and one. The distribution of individual wave heights at the seaward boundary approaches a Rayleigh distribution as  $N \rightarrow \infty$ .

In contrast to the RMS representation, the breaking dissipation is zero for a single wave realization until the Miche incipient breaking criterion is met. Thereafter, the dissipation is assumed to be in proportion to the difference between the wave energy flux and an empirical stable energy flux,  $E_{Fis}$ , associated with a stable wave height of  $0.4d$

$$\overline{D}_{Bi} = \frac{0.15}{d} [E_{Fi} - E_{Fis}] \quad (7)$$

where  $d$  is the still-water depth.

The energy equation (1) is integrated numerically for each offshore wave condition with energy fluxes Equation 5 and breaking dissipation Equation 7 resulting in an estimate of the cross-shore distribution for each individual wave height. The excess momentum fluxes are then expressed as aggregates of the individual cross-shore wave height distributions:

$$S_{xx} = \frac{1}{8} \rho g \left[ n(\cos^2 \alpha + 1) - \frac{1}{2} \right] \frac{1}{N} \sum_{i=1}^N H_i^2 ; \quad S_{xy} = \frac{1}{8} \rho g n \sin \alpha \cos \alpha \frac{1}{N} \sum_{i=1}^N H_i^2 \quad (8)$$

**Predicted wave height compared to laboratory data.** Recent laboratory data of random waves are valuable for model verification. The recirculating Longshore Sediment Transport Facility (LSTF)(Hamilton and Ebersole 2001) was designed for the collection of detailed free surface and velocity data. A total of 110 horizontal measurement positions were set up in the LSTF basin with dimensions of approximately 30 m by 25 m in plan. The analysis of the hydrodynamic and bathymetric conditions over this region demonstrates that the modeling of the tank can justifiably be simplified by assuming alongshore uniformity. The following analysis focuses on a single

cross-shore transect located near the center of the tank. Spilling waves with  $H_{rms} = 18cm$  and peak period  $T_p = 1.5s$  are used as a verification case herein.

The energy equation (1) is solved across the domain using either the RMS or WBW formulation. Random wave fields are characterized by smoothly varying wave heights due to the range of breakpoints, and a first order explicit method is used to numerically integrate Equation 1. This simple procedure is considered to be accurate enough in light of the empirical parameterizations and the smooth variation of energy across the surf zone. Figure 2 shows the cross-shore variation of  $H_{rms}$  for the two formulations as well as laboratory data. The data collection was repeated a total of 10 times resulting in 10 measurements of wave height at each of the 10 cross-shore measurement locations. All of the data are included in Figure 2 to demonstrate the degree of scatter. For each of the numerical solutions, empirical parameters have been chosen based on accepted recommendations, and no attempt has been made to calibrate the models to fit data. The difference between the solutions by these two formulations is due to the unequal breaking dissipation, where the RMS method predicts a larger dissipation in the deeper region of the domain. The RMS method underpredicted the wave height in the outer surf zone, but agreed well with data in the mid-surf. On the other hand, the WBW method matches well with data in the offshore region of the data but overpredicts wave height in the mid- and inner-surf zones.

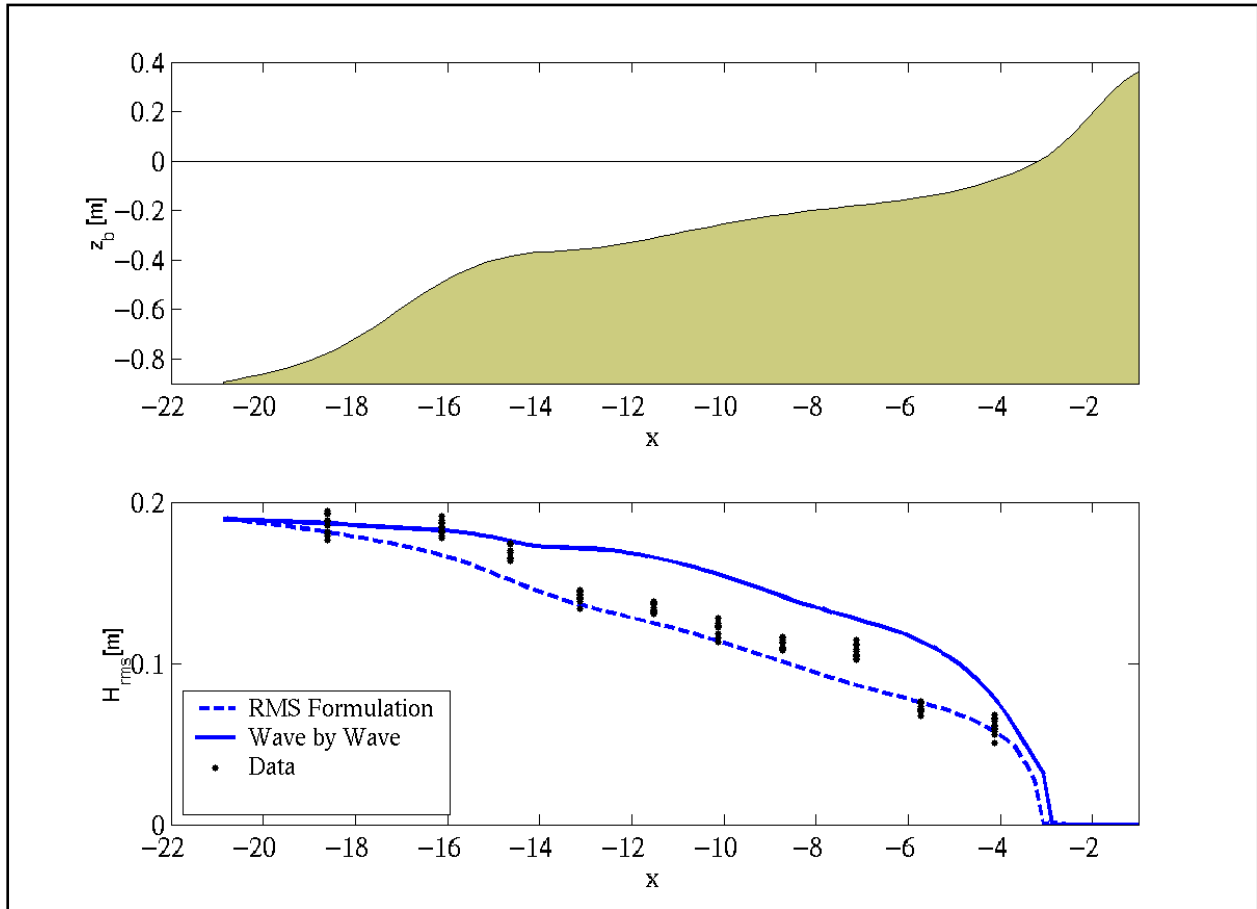


Figure 2. Bathymetry and comparisons of model wave height predictions to measured data

**Cross-Shore Momentum Equation.** The time-averaged cross-shore momentum equation for a long straight coast is given by

$$\overline{\frac{\partial}{\partial x} \int_{z_b}^{\eta} \rho u^2 dz} + \overline{\frac{\partial}{\partial x} \int_{z_b}^{\eta} P dz} - \frac{\rho g}{2} \frac{\partial \bar{h}^2}{\partial x} = -\rho g \bar{h} \frac{\partial \bar{\eta}}{\partial x} + \overline{\frac{\partial}{\partial x} \int_{z_b}^{\eta} \tau_{xx} dz} - \overline{\tau_x^B} \quad (9)$$

where  $u$  is the cross-shore velocity;  $P$  is total pressure;  $\bar{h}$  is the mean water depth;  $\bar{\eta}$  is the mean free-surface position;  $\overline{\tau_{xx}}$  is a Reynolds stress; and  $\tau_x^B$  is the bottom shear stress. The left hand side of Equation 9 is made up of the forcing terms that arise from the organized wave motion as well as current contributions. The time-steady currents may play a role in momentum mixing in the surf zone; it is the case, however, that the rigorous inclusion of these effects is complicated in the trough to crest regions and requires assumptions about the wave shapes and velocity profiles. It is therefore assumed that the currents do not play a vital role, and the velocities in Equation 9 are assumed to be wave induced. Furthermore, it has been shown that the mean bed shear stress and the turbulent mixing are small relative to the forcing and free-surface slope (e.g., Longuet-Higgins and Stewart 1964). Incorporating these simplifications, then, along with a linear representation of the wave induced velocities and pressures yields the familiar cross-shore balance:

$$\frac{\partial S_{xx}}{\partial x} = -\rho g \bar{h} \frac{\partial \bar{\eta}}{\partial x} \quad (10)$$

The momentum equation (10) is then solved numerically for the cross-shore variation of the setup,  $\bar{\eta}$ , given the known radiation stress from Equations 4 or 8. A first-order explicit scheme is considered to be accurate enough for this slowly varying function of cross-shore distance.

To predict the depth variation of the steady cross-shore velocity, use is made of an eddy viscosity closure. The depth-dependent time-averaged cross-shore Reynolds equation is integrated twice vertically to arrive at the variation, and boundary conditions are employed to determine the integration constants and close the problem. It is convenient to decompose the total velocities into steady and time-varying components:

$$u = \bar{u} + \tilde{u} \quad ; \quad v = \bar{v} + \tilde{v} \quad ; \quad w = \bar{w} + \tilde{w} \quad (11)$$

such that all time-varying portions have a diminishing time average i.e.,  $\overline{\tilde{u}} = \overline{\tilde{v}} = \overline{\tilde{w}} = 0$ . It is assumed, in the following, that the steady vertical current  $\bar{w}$  is negligible relative to the horizontal currents. Also, the cross-shore gradients of integrated turbulent shear are assumed to be small (Stive and Wind 1982), and the specification of the vertical gradient of the wave stress  $\overline{\tilde{u}\tilde{w}}$  is given according to Rivero and Arcilla (1995). The equation that governs the current profile, then, is given as

$$\frac{\partial}{\partial z} \left( \nu_{iv} \frac{\partial \bar{u}}{\partial z} \right) = \frac{1}{2} \frac{\partial}{\partial x} (\overline{\tilde{u}^2} - \overline{\tilde{w}^2}) + \frac{\partial}{\partial x} \bar{u}^2 + g \frac{\partial \bar{\eta}}{\partial x} = f_u \quad (12)$$

The simplest solution of the general equation (12) is the specification of a depth-invariant turbulent vertical eddy viscosity  $\nu_{tv}$ . In fact, Garcez Faria et al. (2000) concluded that a depth-dependent eddy viscosity did not improve predictions of the undertow when compared with field data. In the model **NEARHYDS**, the eddy viscosity is expressed as  $\nu_{tv} = 0.01h\sqrt{g\bar{h}}$ . If the forcing  $f_u$  is also considered to be constant over depth, the required two integrations yield a quadratic profile:

$$\bar{u} = \frac{f_u z'^2}{2\nu_{tv}} + \frac{c_1 z'}{\nu_{tv}} + c_2 \quad (13)$$

where  $z' = z + d$  is a new local coordinate system with  $z' = 0$  at the bottom, and  $c_1$  and  $c_2$  can be specified through two boundary conditions. Alternatively, the constants can be determined with one boundary condition and a statement of mass conservation, which is the closure employed in **NEARHYDS**.

The first constant  $c_1$  is expressed through a balance of the bottom shear stress and the eddy viscosity closure with  $\bar{u}|_{z'=0}$ , resulting in  $c_1 = \overline{\tau_{bx}}/\rho$ . The average bottom shear stress is solved with a boundary layer analysis that is beyond the scope of this publication, but combines aspects of Grant and Madsen (1979) with ripple prediction of Nielsen (1992) and wave friction factors outlined by Soulsby (1997). The end result is the determination of a boundary layer thickness  $\delta$  and a shear stress applied to the interior portion of the fluid. The boundary layer solution must be solved iteratively, but it converges within about three iterations.

It is common to determine the second constant with a statement of mass conservation whereby a finite mass flux due to the presence of waves is balanced by a steady seaward directed current under the trough level. Kennedy et al. (1998) approximated the volume flux through the time averaged continuity equation and linear long wave resulting in an expression for the average undertow below trough level:

$$\bar{u}_r = -\frac{\sqrt{g\bar{h}}}{8} \left( \frac{H_{rms}}{\bar{h}} \right)^2 \cos \alpha \quad (14)$$

The final unknown can then be determined by equating the mass flux and the assumed form of  $\bar{u}$  expressed in Equation 13 integrated from the bed to the trough level, resulting in

$$c_2 = \bar{u}_r - \frac{f_u}{6\nu_{tv}} d_t^2 - \frac{\overline{\tau_{bx}}}{2\nu_{tv} \rho} d_t \quad (15)$$

where  $d_t$  is the distance from the bed to the trough level, approximated as  $h - \frac{H_{rms}}{2}$ . Substitution of the constants into Equation 13 yields

$$\bar{u} = \bar{u}_r + \frac{1}{2\nu_{tv}} \frac{\partial}{\partial x} \left\{ \frac{\bar{u}^2}{2} - \frac{\bar{w}^2}{2} + \bar{u}_r^2 + g\bar{\eta} \right\} \left\{ z'^2 - \frac{d_t^2}{3} \right\} + \frac{\overline{\tau_{bx}}}{\nu_{tv} \rho} \left\{ z' - \frac{d_t}{2} \right\} \quad (16)$$

where  $\bar{u}$  is approximated as  $\bar{u}_r$  in the formulation of  $f_u$ .

The solution of the undertow problem requires the specification of the so-called radiation stress terms  $\bar{u}^2$  and  $\bar{w}^2$  in Equation 16. The simplest solution is the use of depth invariant linear long-wave forcing

$$\tilde{u} = \sqrt{\frac{g}{h}} \tilde{\eta} \quad ; \quad \tilde{w} = \sqrt{\frac{g}{h}} \frac{\partial \tilde{\eta}}{\partial x} z' \quad (17)$$

One of the stress terms, for example, is then expressed as

$$\bar{u}^2 = \frac{g}{h} \overline{\tilde{\eta}^2} = \frac{g}{h} \frac{H_{rms}^2}{8} \quad (18)$$

where  $H_{rms} = \sqrt{8}\sigma$  has been used.

Thus the depth variation of the steady cross-shore flow is solved with the use of a local mass conservation, a shear stress boundary condition, and linear long-wave theory to quantify radiation stresses.

**Alongshore Momentum Equation.** The time-averaged momentum equation for a long straight coast is a balance of the organized wave forcing and current momentum with turbulent mixing and bottom shear stress.

$$\frac{\partial}{\partial x} \overline{\int_{z_b}^{\eta} \rho uv \, dz} = \frac{\partial}{\partial x} \overline{\int_{z_b}^{\eta} \tau_{xy} \, dz} - \overline{\tau_y^B} \quad (19)$$

where  $v$  is the longshore current. The left-hand-side of Equation 19 represents the combined effects of wave forcing and current dispersion. As in the cross-shore momentum equation, the steady currents may play a role in the distribution of momentum in the surf zone. These effects are neglected, however, due to the added complexity and ambiguities associated with a more detailed analysis. The assumption, therefore, is that the current effects are small, and that the wave-induced forcing dominates this term and can be quantified with linear theory:

$$\overline{\int_{z_b}^{\eta} \rho uv \, dz} \approx \overline{\int_{z_b}^{\eta} \rho \tilde{u} \tilde{v} \, dz} = S_{xy} \quad (20)$$

where  $S_{xy}$  is the radiation stress given by Equations 4 or 8.

A common Reynolds-type expression is employed in the specification of the mixing term and it is assumed that the mixing stress can be expressed in terms of the near-bottom velocity gradient. The eddy viscosity  $\nu_t$  is typically assumed to be depth invariant for the solution of the alongshore momentum problem, and then the mixing shear term in Equation 19 is expressed:

$$\frac{\partial}{\partial x} \int_{z_b}^{\eta} \overline{\tau_{xy}} dz = \frac{\partial}{\partial x} \left( \rho h \nu_t \frac{\partial \overline{v_\delta}}{\partial x} \right) \quad (21)$$

The eddy viscosity  $\nu_t$  is expressed as in Longuet-Higgins (1970),  $\nu_t = N |x_{sws}| \sqrt{gh}$  where  $N$  is an empirical dimensionless coefficient, and  $|x_{sws}|$  is the distance to the shoreline.

While the bottom shear stress could justifiably be neglected in the depth integrated cross-shore momentum balance, the near bed stress is the primary force counteracting the radiation stress gradient in the longshore balance. Use is made of the quadratic friction law to define the time-averaged stress

$$\overline{\tau_y^B} = \rho c_f |\overline{u_\delta}| \overline{v_\delta} \quad (22)$$

where the subscript  $\delta$  indicates that the velocities are taken near the bottom but outside of the boundary layer. The time-averaging in Equation 22 is complicated by the necessary detailed knowledge of magnitudes and phasing for both the steady and time-varying velocities. Consequently, the square wave approximation of Nishimura (1982) is employed to give a simplified expression for the shear stress. In the interest of brevity, the equations are not presented.

Utilizing the previous simplifications, Equation 19 reduces to

$$\frac{\partial}{\partial x} S_{xy} = \frac{\partial}{\partial x} \left( \rho h \nu_t \frac{\partial \overline{v_\delta}}{\partial x} \right) - \overline{\tau_y^B} \quad (23)$$

The simplified alongshore momentum equation thus reduces to a second-order differential equation. Central differences are used to solve for the near-bed longshore velocity  $\overline{v_\delta}$  with known radiation stresses. A central difference representation of the mixing term necessitates the solution of Equation 23 as a system of implicit linear finite-difference equations. The offshore boundary condition is specified by the user, and the shoreline boundary condition is developed by solving Equation 23 without momentum mixing. Note that the undertow solution must be completed prior to an along-shore momentum balance due to the inclusion of the cross-shore velocity in the bottom shear stress formulation.

As in the cross-shore flow, prediction of the depth variation of the steady longshore velocity is made with the use of an eddy viscosity closure. The depth-dependent time-averaged alongshore Reynolds equation is integrated twice vertically to determine the steady current profile. Boundary conditions are then employed to determine the constants of integration. Stive and Wind (1982) demonstrated that the horizontal turbulent stress term was small, and thus it is neglected. Also, the vertical wave-induced flows are assumed to be phase shifted relative to the horizontal flows such that  $\overline{\tilde{v}\tilde{w}}$  is small. Neglecting the steady term that includes the steady vertical current is justifiable for small bottom slopes, and the simplified equation that governs the current profile is expressed

$$\frac{\partial}{\partial z} \nu_{tv} \frac{\partial \bar{v}}{\partial z} = \frac{\partial}{\partial x} \{ \bar{u}_r \mathbf{V} + \bar{v}\bar{u} \} \quad (24)$$

Where  $\mathbf{V}$  is the depth-averaged longshore velocity under the trough level. Again, the right-hand-side of Equation 24 is made up of current and wave forcing components and is assumed to be independent of depth. The implicit nature of this equation dictates the iterative solution employed in **NEARHYDS**. Proceeding as in the cross-shore problem, Equation 24 is integrated twice, generating two constants of integration. As previously, the eddy viscosity is assumed to be depth-uniform and identical to the formulation used in the undertow problem. The first constant is specified with the match of turbulent stress and the bottom shear stress obtained from the solution of the depth-integrated alongshore momentum equation (23). The second constant is determined from the computed near-bottom velocity  $\bar{v}_\delta$  resulting in

$$\bar{v} = \bar{v}_\delta + \frac{1}{2\nu_{tv}} \frac{\partial}{\partial x} \{ \bar{u}_r \mathbf{V} + \bar{v}\bar{u} \} z'^2 + \frac{\bar{\tau}_y^B}{\rho\nu_{tv}} z' \quad (25)$$

where the short-wave forcing term  $\bar{v}\bar{u}$  is quantified according to linear long-wave theory.

**PREDICTED NEARSHORE CURRENTS COMPARED TO LAB DATA:** The LSTF test case of spilling waves that was used for the comparison of predicted wave heights to data is also used to gauge the accuracy of the computed setup as well as predicted current magnitudes and depth profiles. The waves with an offshore wave angle of 10 deg generated a longshore current and a seaward directed return current over the movable bed. A time series of velocities was collected at 10 positions throughout the water column at each cross-shore position as shown in Figure 3. The portion of the column covered by the dense vertical spacing of measurement locations is used to verify the cross-shore and longshore current models. The nearshore currents were computed using standard values for the coefficient of friction  $c_f = 0.01$  and the horizontal mixing coefficient  $N = 0.04$ . No attempt has been made to achieve a better fit with data by tailoring these factors.

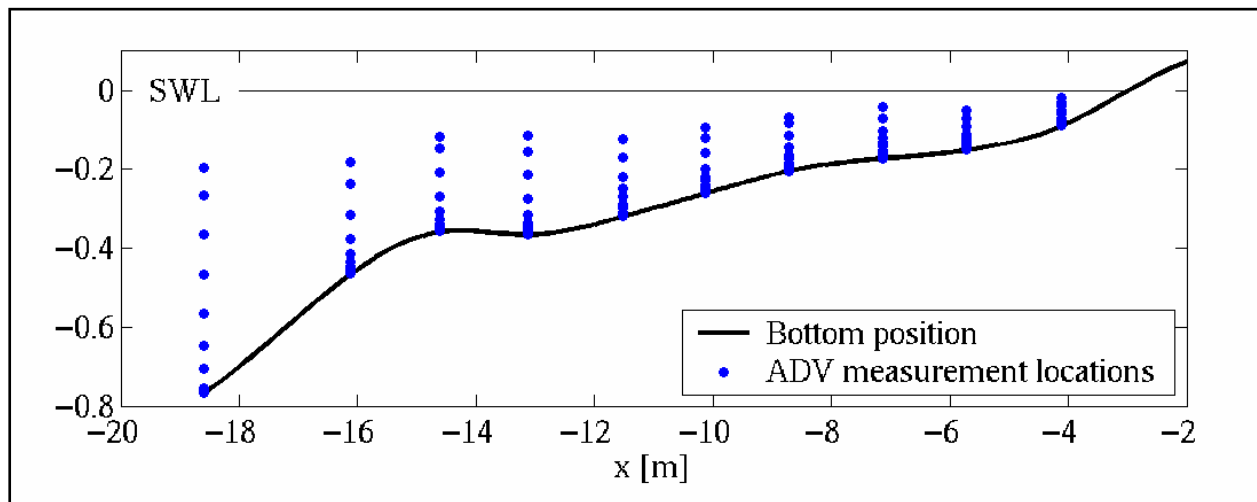


Figure 3. Vertical measuring locations Test 1H, case 3

The time-average surface position is shown in Figure 4. As in the presentation of the wave height data, all of the measurements are shown at each position in order to demonstrate the degree of scatter. The differences in the RMS and WBW methods are consistent with the previously shown wave height computations considering that mean free-surface slope is a result of the decay in  $H_{rms}$ . It is expected, then, that the RMS formulation will exhibit a greater setup through most of the domain; the greatest slope in the mean free-surface for the WBW method, on the other hand, will be in the nearshore where the wave heights drop off quickly.

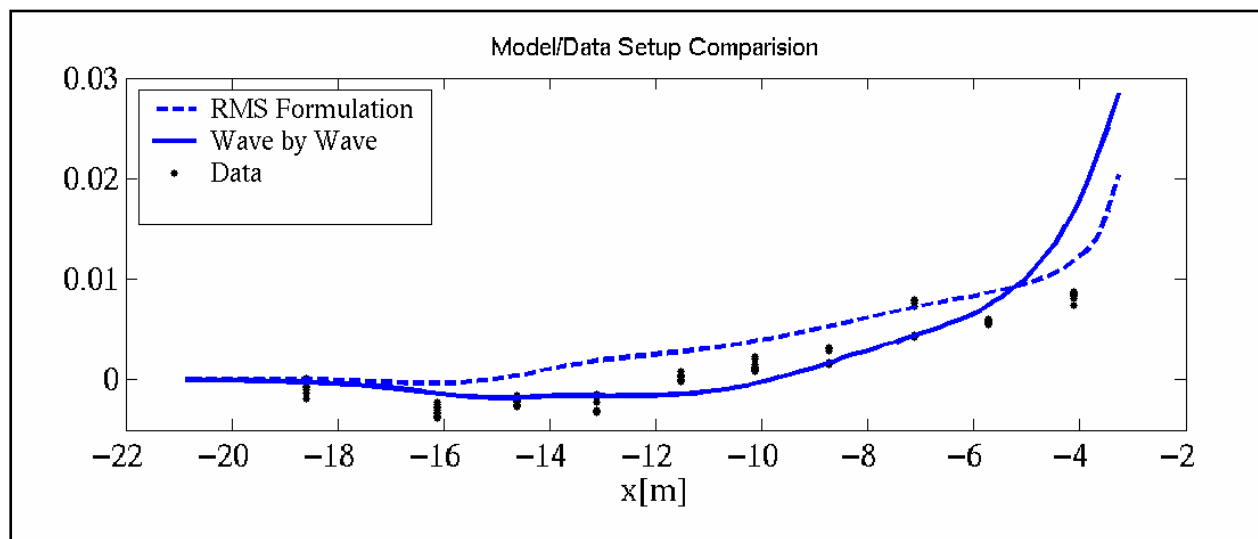


Figure 4. Mean free-surface position data and predictions

The model predictions for the magnitude and profile of the undertow are compared with data measured at 10 cross-shore locations in Figure 5. The problems of accurate undertow prediction are compounded by a reliance on the total mass flux parameterization, which, in turn, is dependent on the solution of the energy equation. Despite this challenge, the undertow magnitude predictions of the model compare well with the measured data. The shape of the current profile is also predicted well with differences between the WBW and RMS methods due to the contrasting cross-shore distributions of wave height and associated radiation stresses.

Computed and measured steady longshore currents are shown in Figure 6. The model uses the measured (and negative) longshore velocity at the first measurement location as a seaward boundary condition. It is interesting to note, however, that the specification of a non-zero boundary condition on the seaward boundary has only a localized effect. The only mechanism for non-local generation and dissipation of longshore current is due to the momentum mixing, and the influence of the seaward boundary drops off with a weak mixing effect. The profile is well predicted with NEARHYDS and the difference between the WBW and RMS formulations is small.

**SUMMARY:** The model NEARHYDS solves the phase-averaged energy equation to determine the cross-shore distribution of RMS wave heights and the associated radiation stresses. In turn, the wave stresses act as a forcing mechanism in the depth-integrated cross-shore and alongshore momentum

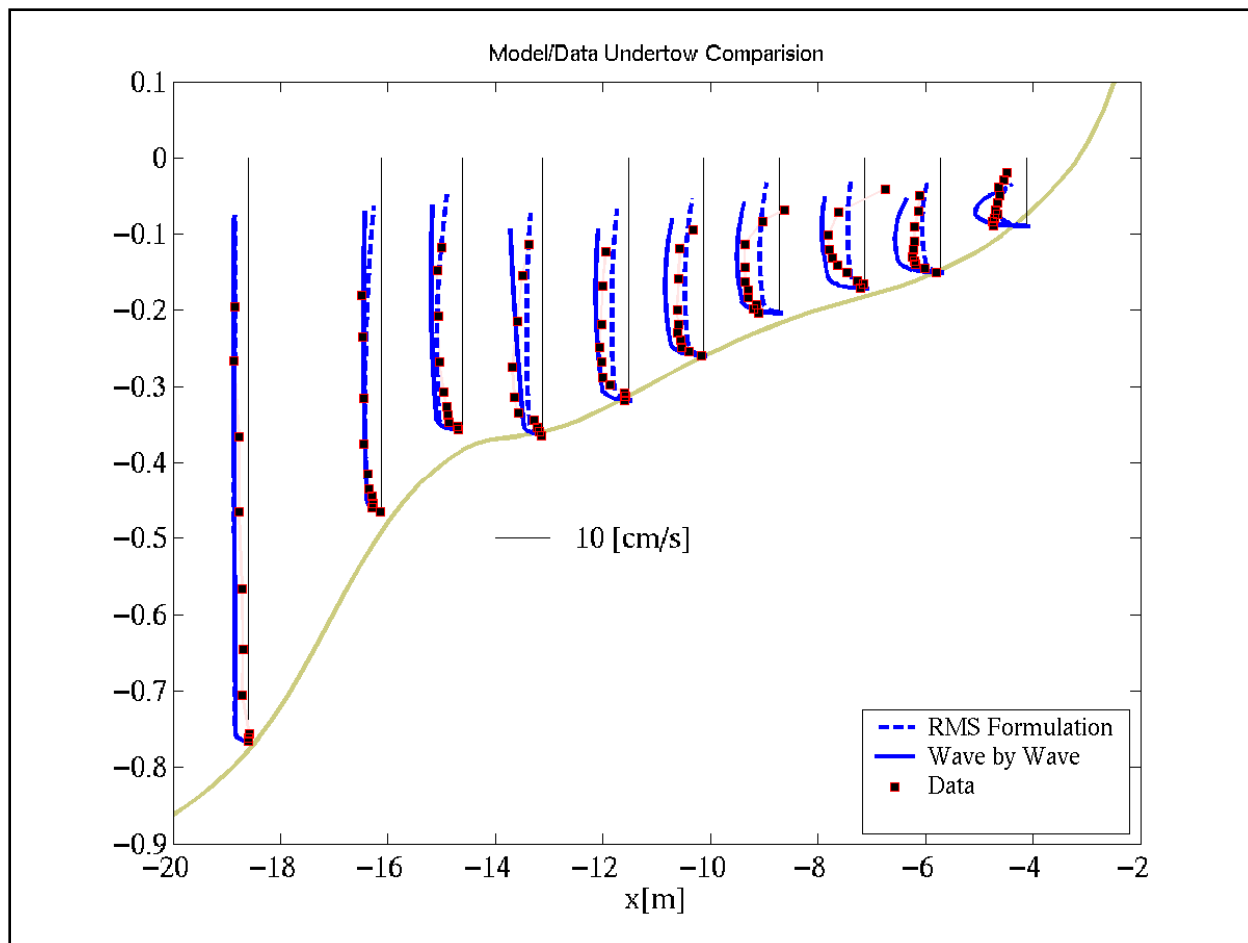


Figure 5. Undertow data and predictions

equations that include mixing and bottom friction. Finally, with use of the previously described analyses, the depth variation of the currents can be determined based on the horizontal Reynolds equations.

The prediction of wave height is shown to differ based on the choice of RMS or WBW formulations, although both methods predict  $H_{rms}$  reasonably well. The differences in the computed setup are consistent with the varied wave height predictions. The longshore current computations agree well with data both in magnitude and profile shape. The undertow predictions, on the other hand, show greater error when compared with data. Additionally, the undertow profile is shown to be sensitive to the solution of the energy equation.

Model input requirements include 1-D (cross-shore) bathymetry and incident wave parameters ( $H_{rms}, T_p, \alpha$ ). Options include RMS or WBW formulations, bottom friction formulation, mixing coefficients, as well as other solution parameters. **NEARHYDS** computes the cross-shore distribution of wave height and setup. Additionally, the steady cross-shore and depth dependent current fields are computed. Model output is displayed graphically and is recorded to ASCII files. The graphical user interface is intended to make **NEARHYDS** intuitive and simple to use.

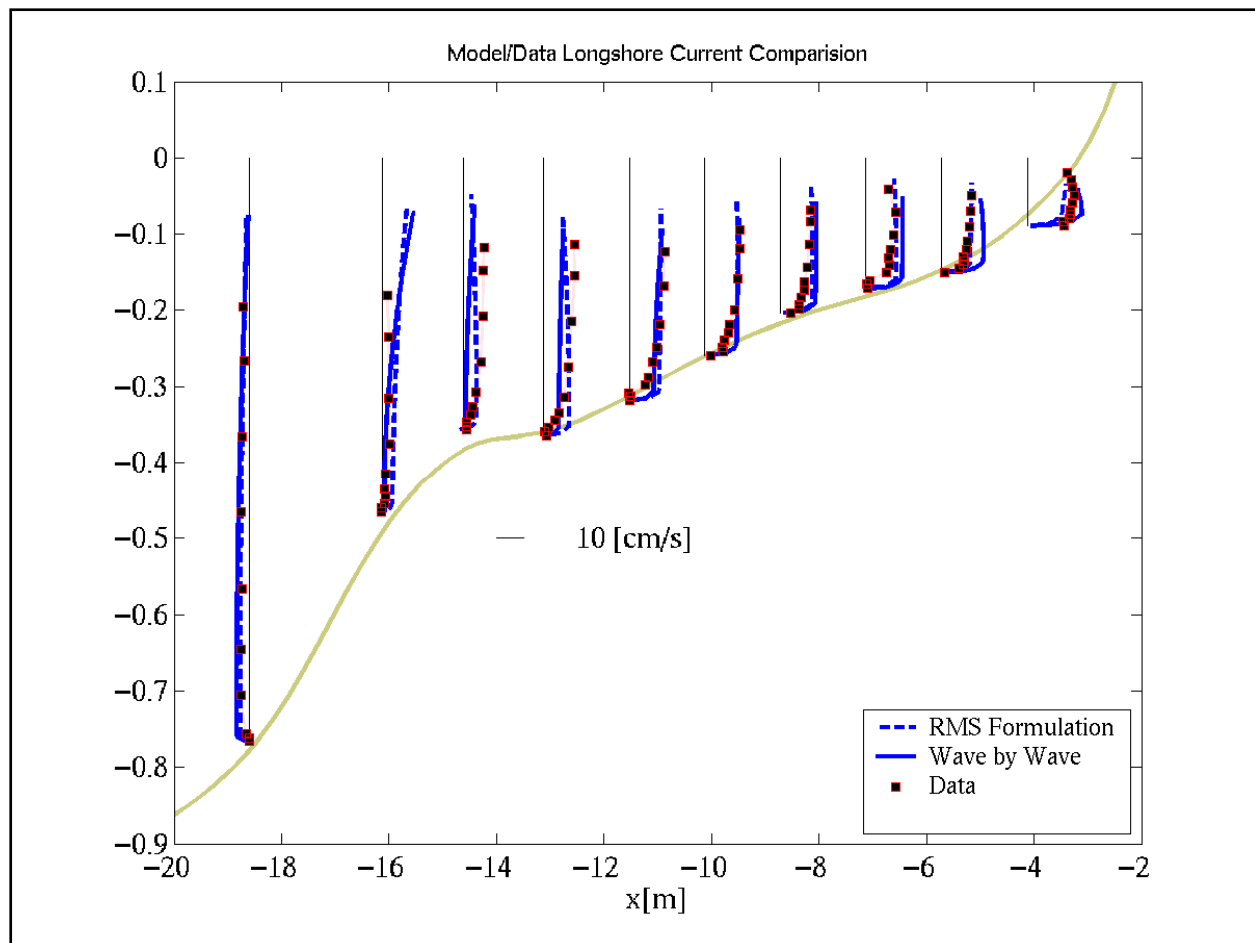


Figure 6. Longshore current data and predictions

**POINT OF CONTACT:** For additional information, or to obtain a copy of the model, contact Dr. Bradley Johnson, Coastal Processes Branch, Coastal and Hydraulics Laboratory, U.S. Army Engineer Research and Development Center, Vicksburg, MS 39180. Voice: 601-634-4612, FAX: 601-634-4314 email: [Bradley.D.Johnson@erdc.usace.army.mil](mailto:Bradley.D.Johnson@erdc.usace.army.mil).

## REFERENCES

- Battjes, J. A. (1974). "Computation of set-up, longshore currents, runup and overtopping due to wind generated waves," *Communications on hydraulics*. Delft University of Technology Report 74-2.
- Battjes, J. A., and Janssen, J.P.F.M. (1978). "Energy loss and set-up due to breaking of random waves," *Proc. of the 16<sup>th</sup> Coastal Engineering Conference*, ASCE, 569-587.
- Battjes, J. A., and Stive, M.J.F. (1985). "Calibration and verification of a dissipation model for random breaking waves," *J. of Geophysical Research* 90(C5), 9159-9167.
- Bowen, A. J. (1969). "The generation of longshore currents on a plane beach," *J. Marine Research* 27, 206-215.
- Dally, W. R. (1992). "Random breaking waves: Field verification of a wave-by-wave algorithm for engineering application," *J. Coastal Engineering* 16, 369-397.

- Garcez Faria, A. F., Thornton, E. B., Lippmann, T. C., and Stanton, T. P. (2000). "Undertow on a barred beach," *J. Geophysical Research* 105(C7) 16999–17010.
- Grant, W. D., and Madsen, O. S. (1979). "Combined wave and current interaction with a rough bottom," *J. Geophysical Research* 84(C4), 1797–1808.
- Hamilton, D. G., and Ebersole, B. A. (2001). "Establishing uniform longshore currents in a large-scale laboratory facility," *J. Coastal Engineering* 42, 199–218.
- Karambas, T. V., and Koutitas, C. (2002). "Surf and swash zone morphology evolution induced by nonlinear waves," *J. Waterway, Port, Coastal, and Ocean Engineering* 128(3) 102–113.
- Kennedy, D. L., Cox, D. T., and Kobayashi, N. (1998). "Application of an undertow model to irregular waves on barred beaches and reflective coastal structures," *Proc. of 26<sup>th</sup> Coast. Eng. Conference*, ASCE 311–324.
- Kobayashi, N., and Johnson, B. D. (2001). "Sand suspension, storage, advection and settling in surf and swash zones," *J. Geophysical Research* 106(C5) 9363–9376.
- Kraus, N. C., and Larson, M. (1991). "NMLong: numerical model for simulating the longshore current," *Technical Report DRP-91-1*, U.S. Army Corps of Engineers.
- Lin, P., and Liu, P. L. -F. (1998). "Turbulence transport, vorticity dynamics, and solute mixing under plunging breaking waves in surf zone," *J. of Geophysical Research* 103(C8), 15677–15694.
- Longuet-Higgins, M. S. (1970). "Longshore currents generated by obliquely incident sea waves. Parts 1 and 2," *J. of Geophysical Research* 75, 6778–6801.
- Longuet-Higgins, M. S., and Stewart, R. W. (1964). "Radiation stresses in water waves: A physical discussion, with applications," *Deep Sea Research* 11, 529–562.
- Nielsen, P. (1992). *Coastal Bottom boundary layers and sediment transport*. World Sci., River Edge, NJ.
- Nishimura, H. (1982). "Numerical simulation of nearshore circulation." *Proc. of 29<sup>th</sup> Japanese Conference of Coastal Engineering*, Japanese Society of Civil Engineers, 333–337 (in Japanese).
- Rivero, F. J., and Arcilla, A. S. (1995). "On the vertical distribution of  $\langle \tilde{u}\tilde{v} \rangle$ ." *Coastal Engineering* 25, 137–152.
- Soulsby, R. L. (1997). *Dynamics of marine sands*. Thomas Telford, London, UK.
- Stive, M. J. F., and Wind, H. G. (1982). "A study of radiation stress and set-up in the nearshore region," *Coastal Engineering* 6, 1–25.
- Thornton, E. B., and Guza, R. T. (1986). "Surf zone longshore currents and random waves: Field data and models," *J. Physical Oceanography* 16, 1165–1178.

**NOTE:** The contents of this technical note are not to be used for advertising, publication, or promotional purposes. Citation of trade names does not constitute an official endorsement or approval of the use of such products.